J. Fluid Mech. (1987), *vol.* 185, *pp.* 107–120
Printed in Great Britain

Topographic waves in rectangular basins

By THOMAS STOCKER AND KOLUMBAN HUTTER
Laboratory of Hydraulics, Hydrology and Glaciology, 8092-ETH Zürich, Switzerland

(Received 15 July 1986 and in revised form 13 April 1987)

The channel model of Stocker & Hutter (1986, 1987) is used to construct topographic wave solutions in a rectangular basin on the f-plane with variable but symmetric bathymetry. We show that in a narrow period band three types of eigenmodes can be discerned which exhibit local, midscale and global structure, respectively. Wave motion can be trapped either at the long sides of the elongated basin (channel mode) or at the ends of it (bay mode) or alternatively, a basinwide phase rotation is observed (Ball mode). The new bay modes are explained as resonances of topographic wave reflection in a semi-infinite channel. The influence of the variation of the aspect ratio of the rectangle and the topography parameter on the wave periods is also investigated.

1. Introduction

Long-periodic signals in temperature– and velocity–time series recorded by moored instruments in the Great Lakes (Saylor, Huang & Reid 1980), the Lake of Lugano (Hutter, Salvadè & Schwab 1983; Mysak *et al.* 1985) and the Lake of Zürich (Hutter & Vischer 1986) have been attributed to topographic waves; an overview is given in Stocker & Hutter (1987).

Second-class motions have been studied analytically in some special domains: Lamb (1932) studied a circular basin with parabolic depth profile, and extensions thereof were presented by Saylor *et al.* (1980); elliptical basins were investigated by Ball (1965), Mysak (1985) and Johnson (1987*a*). In a recent paper by Johnson (1987*b*) a solution technique is presented which allows calculation of eigenmodes in semi-infinite channels and elongated basins with smooth boundaries. All these models showed mode features which could be well identified in the observations. Furthermore, by adequately adjusting the free parameters in these models, the theoretical periods could be brought into close proximity to the periods deduced from the measured time series. An outstanding feature of these solutions is their global nature: water particles in the entire lake basin are in motion, and the gyres extend over a substantial portion of the basin. As a result, the trace of the topographic wave could be detected almost everywhere in the basin.

While the analytical results of the circular and elliptical basins yield wave structures which are at least in qualitative agreement with observations, it must be admitted that the bathymetry of the real basins is not closely approximated in these cases. This is why the topographic wave equation has been numerically solved for the Lake of Lugano by the finite element method (Trösch 1984) with results which do not at all support the interpretation using models known so far. He finds that solutions in the 65- to 95-hour period range are localized to the two narrow ends and the Bay of Lugano, whereas the majority of the basin remains unaffected. Thus we ask: Are these long periodic phenomena indeed interpretable as topographic waves?

On the other hand numerical finite difference computations for channels (Bäuerle 1986; Bäuerle & Hutter 1987, paper in preparation) have indicated that an unusually high resolution of the discretized topographic wave equation is needed to calculate accurately the dispersion relation. This favours spectral methods and suggests the use of ODE-integrators because with them high-accuracy forward and multi-step integration is possible.

To overcome the limitations and difficulties associated with idealized basins and numerical solutions we introduce an alternative procedure. Using the Method of Weighted Residuals (Finlayson 1972), by expanding the mass transport stream function along the narrow direction of an elongated basin in terms of a complete set of shape functions with unknown coefficients, we transform the topographic wave operator into an ODE-operator for the unknown coefficient functions.

Section 2 introduces the governing equations and explains this transformation. Numerical solutions of topographic waves are collected in §3.1, their convergence and parameter properties are investigated in §3.2. A physical interpretation of the new bay type is given in §3.3.

2. Mathematical model

Conservation of mass and angular momentum in a rotating homogeneous fluid under no external forces can be expressed by stating that the potential vorticity of each fluid particle be conserved. With the mass transport stream function ψ, and extracting a harmonic time dependence $e^{-i\omega t}$ and employing the rigid-lid assumption, this yields the boundary-value problem

$$\left.\begin{aligned} -i\omega\nabla\cdot\left(\frac{\nabla\psi}{H}\right)+\hat{z}\cdot\left(\nabla\psi\times\nabla\frac{f}{H}\right)=0 \quad &\text{in } \mathscr{D}, \\ \psi=0 \quad &\text{on } \partial\mathscr{D}, \end{aligned}\right\} \tag{2.1}$$

where H is the water depth, f the Coriolis parameter, ω the frequency, ∇ the horizontal gradient operator, $\hat{z}$ a unit vector in the direction opposite to gravity, and $\mathscr{D}$ is the lake domain with boundary $\partial\mathscr{D}$, through which no mass flux is assumed. The vertically averaged velocity field $\boldsymbol{u}$ is obtained from (2.1) via the formula

$$\boldsymbol{u}=\frac{1}{H}(\hat{z}\times\nabla\psi). \tag{2.2}$$

Henceforth (2.1) will be used in dimensionless form. Horizontal lengths will be scaled with L_0, depth with H_0 and frequencies with the Coriolis parameter which will be assumed to be constant (f-plane). Thus (2.1) transforms to

$$\left.\begin{aligned} -i\sigma\nabla\cdot\left(\frac{\nabla\psi}{H}\right)+\hat{z}\cdot\left(\nabla\psi\times\nabla\frac{1}{H}\right)=0 \quad &\text{in } \mathscr{D}, \\ \psi=0 \quad &\text{on } \partial\mathscr{D}, \end{aligned}\right\} \tag{2.3}$$

where $\sigma=\omega/f$ and all variables and operators are now dimensionless. We further assume that the topography of the rectangular basin is symmetric with respect to its middle axis, i.e. $H(s,n)=H(s,-n)$, $B^+(s)=-B^-(s)\equiv\frac{1}{2}B(s)$. We identify it with the s-axis of the natural coordinate system (s, n, z) choosing the origin at one end of the basin, see figure 1.

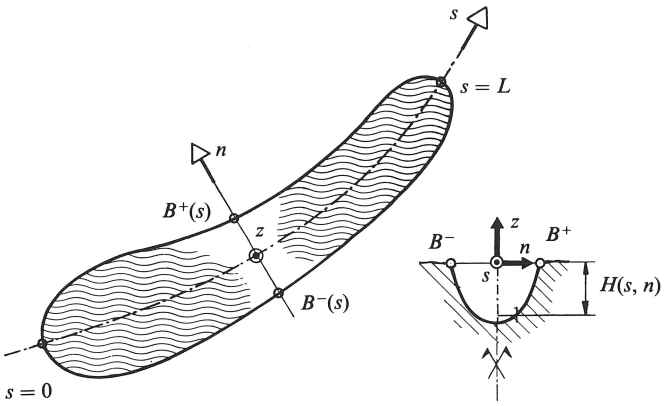

FIGURE 1. Elongated lake and transverse section in a natural (s, n, z)-coordinate system. The thalweg axis ($n = 0$) may be a centre of symmetry and have curvature $K(s)$.

The basin is long in the s-direction and narrow in the n-direction. This suggests solving (2.3) by the shape function expansion

$$\psi(s,n) = \sum_{\alpha=1}^{N} P_\alpha^+(s,n)\,\psi_\alpha^+(s) + \sum_{\alpha=1}^{N} P_\alpha^-(s,n)\,\psi_\alpha^-(s), \tag{2.4}$$

where $P_\alpha^\pm(s,n)$ are symmetric and antisymmetric preselected functions with respect to n and $\psi_\alpha^\pm(s)$ are unknown coefficient functions. For instance

$$\left.\begin{aligned} P_\alpha^+(s,n) &= \cos\left(\pi(\alpha-\tfrac{1}{2})\frac{2n}{B(s)}\right) \\ P_\alpha^-(s,n) &= \sin\left(\pi\alpha\frac{2n}{B(s)}\right) \end{aligned}\right\} \quad (\alpha = 1, \ldots, N), \tag{2.5}$$

in which $B(s)$ is the scaled width of the symmetric basin. When the rectangle B is constant, the curvature K vanishes, and we adopt the profile

$$H(s,n) = h(s)\left(1+\epsilon-\left|\frac{2n}{B}\right|^q\right) \quad (0 < s < L, \quad -\tfrac{1}{2}B < n < \tfrac{1}{2}B), \tag{2.6}$$

with constant ϵ and q $(0 < q < \infty)$. This bathymetry possesses a finite shore depth $\epsilon h(s)$, which is necessary to have $(\partial H/\partial n)/H$ bounded everywhere.

Stocker & Hutter (1986, 1987) explained in detail how the boundary-value problem (2.3) is transformed to a new two-point boundary-value problem for the coefficient functions $\psi_\alpha^\pm(s)$ in (2.4). This is achieved by a weighted integration of (2.3) over the small direction and the result is

$$\left.\begin{aligned} \mathbf{M}\boldsymbol{\psi}(s) &= \mathbf{0} \quad (0 < s < L), \\ \boldsymbol{\psi}(s) &= \mathbf{0} \quad (s = 0, L), \end{aligned}\right\} \tag{2.7}$$

in which

$$\left.\begin{aligned} \boldsymbol{\psi} &= (\psi_1^+, \ldots, \psi_n^+;\ \psi_1^-, \ldots, \psi_n^-) = (\boldsymbol{\psi}^+; \boldsymbol{\psi}^-), \\ \mathbf{M} &= -\mathrm{i}\sigma\left[B^2\boldsymbol{K}^{00}\frac{\mathrm{d}^2}{\mathrm{d}s^2} - B^2\left(h^{-1}\frac{\mathrm{d}h}{\mathrm{d}s}\right)\boldsymbol{K}^{00}\frac{\mathrm{d}}{\mathrm{d}s} - \boldsymbol{K}^{22}\right] \\ &\quad - B(\boldsymbol{K}^{20}+\boldsymbol{K}^{02})\frac{\mathrm{d}}{\mathrm{d}s} + B\left(h^{-1}\frac{\mathrm{d}h}{\mathrm{d}s}\right)\boldsymbol{K}^{20}. \end{aligned}\right\} \tag{2.8}$$

Evidently, $\mathbf{M}$ is a second-order matrix differential operator and $\boldsymbol{K}^{00}$, etc. are $2N \times 2N$ real matrices whose entries depend on ϵ and q; these are given in Stocker & Hutter (1987). Moreover, $\mathbf{M}$ has constant coefficients whenever $h^{-1}(\mathrm{d}h/\mathrm{d}s) = \text{constant}$. Here it is assumed that $\mathbf{M}$ varies with s through an arbitrary thalweg depth $h(s)$.

With the truncated expansion (2.4) an approximation is introduced, but it is hoped that, by an appropriate selection of the shape functions $P_\alpha^{\pm}(s, n)$, one can keep the order N of the model small. We shall see that in practice $N = 2$ is often sufficient. Problem (2.7) only contains one spatial dimension and, therefore, permits use of a fourth-order Runge–Kutta scheme.

For the numerical solution it is advantageous to transform (2.7) to standard form. With

$$\boldsymbol{\Psi} \equiv (\mathrm{Re}\,\boldsymbol{\psi}^+, \mathrm{Re}\,\boldsymbol{\psi}^-, \mathrm{Re}\,\dot{\boldsymbol{\psi}}^+, \mathrm{Re}\,\dot{\boldsymbol{\psi}}^-; \mathrm{Im}\,\boldsymbol{\psi}^+, \mathrm{Im}\,\boldsymbol{\psi}^-, \mathrm{Im}\,\dot{\boldsymbol{\psi}}^+, \mathrm{Im}\,\dot{\boldsymbol{\psi}}^-),$$

$$(\,)^{\cdot} \equiv \frac{\mathrm{d}}{\mathrm{d}s},$$

(2.7) corresponds to the real system

$$\left.\begin{aligned} &\frac{\mathrm{d}}{\mathrm{d}s}\boldsymbol{\Psi} = \boldsymbol{A}(s)\boldsymbol{\Psi} \quad (0 < s < L), \\ &\boldsymbol{B}\boldsymbol{\Psi} = \mathbf{0} \qquad\quad (s = 0, L). \end{aligned}\right\} \tag{2.9}$$

This system has the dimension $8N$; $\boldsymbol{B}$ is a diagonal matrix with $B_{ii} = 1$ for $i = 1, \ldots, 2N$ and $i = 4N+1, \ldots, 6N$, or else $B_{ii} = 0$, and $\boldsymbol{A}$ is a $8N \times 8N$ matrix which can easily be computed from $\mathbf{M}$.

Solutions of (2.9) were constructed numerically for the lake-axis depth profile

$$h(s) = \eta + \sin^p\left(\frac{\pi s}{L}\right) \quad (p > 1), \tag{2.10}$$

here with $p = 2$. η and p are parameters; $\eta > 0$ guarantees that the depth is never zero and the exponent p could be varied such that the longitudinal variation of the depth is more or less concentrated at the long ends of the lake.

3. Numerical results

In what follows, numerical solutions will be discussed without going into any details of computational peculiarities. Emphasis will be on the physical interpretation.

3.1. *A new type of topographic wave*

We investigate the spectrum of topographic waves in a second- and a third-order model, i.e. $N = 2$ and $N = 3$. The basin is rectangular with an aspect ratio $r = 0.5$, a parabolic cross-section ($q = 2.0$) and a thalweg varying as $(\sin)^2$. Figures 2 and 3 display a selection of modes from the spectrum of a second- and a third-order model, respectively. It is apparent that in the period interval from 35 h to 140 h (corresponding to 45° latitude) a large variety of qualitatively different eigenmodes can be detected. According to the complexity of their modal structure we distinguish three types of eigenmodes.

Type 1 is the well-known modal pattern described by all exact models of topographic waves in enclosed basins. It is akin to Ball's solutions (Ball 1965) and therefore called *Ball-type*. Both the linear ($\sigma = 0.155$) and the quadratic ($\sigma = 0.213$)

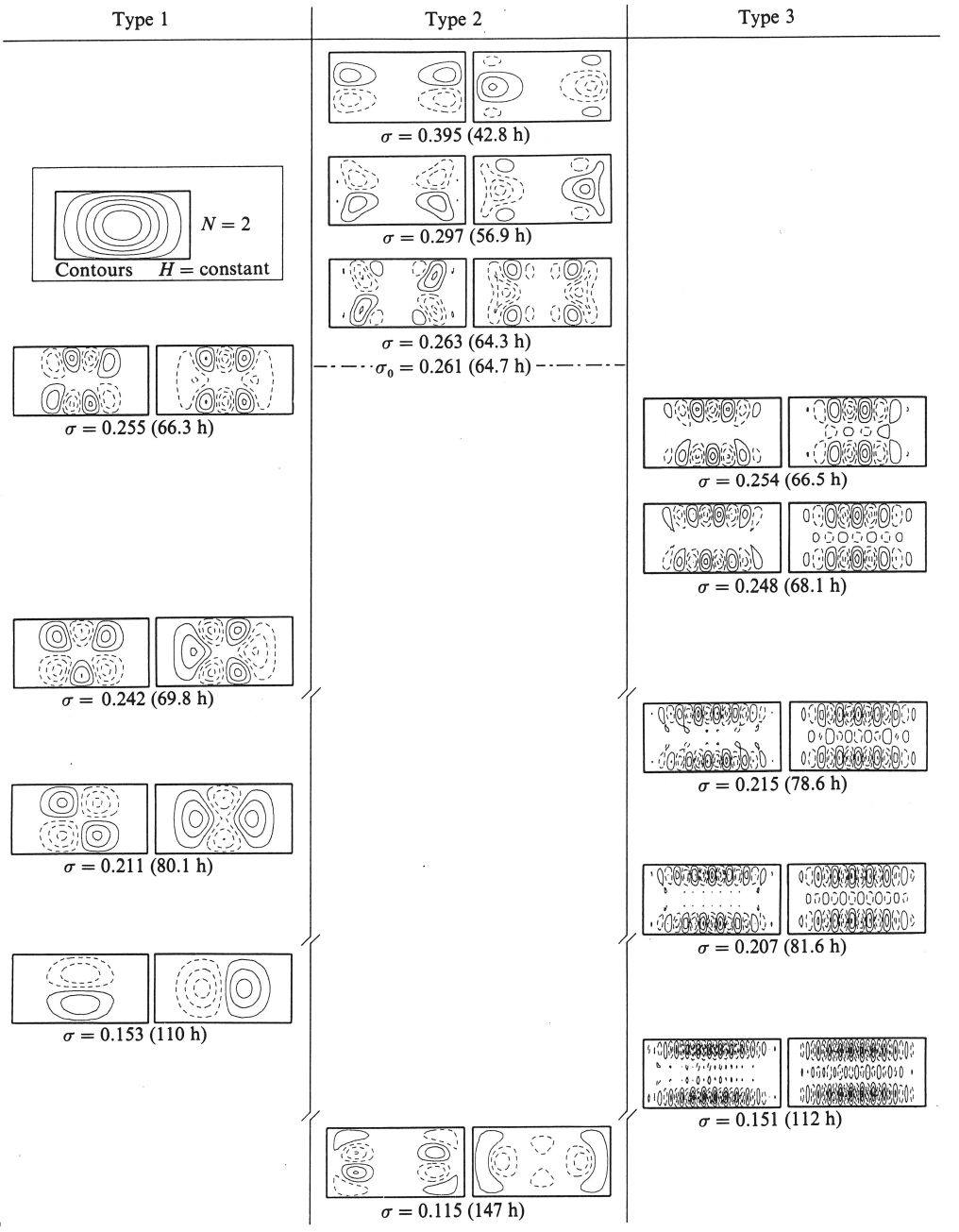

FIGURE 2. Selection through the spectrum of topographic wave modes in a second-order model. The eigenfrequencies increase towards the top of the figure. The contour lines of ψ are plotted for time $t = 0$ (left) and $t = \frac{1}{4}T$ (right). Three types of solution can be distinguished and cuts of the vertical lines indicate further modes not shown here. The parameters are: $N = 2$, $r = 0.5$, $q = 2.0$, $\epsilon = 0.05$, $\eta = 0.01$ and $f = 2\pi/16.9\,\mathrm{h}$ has been used.

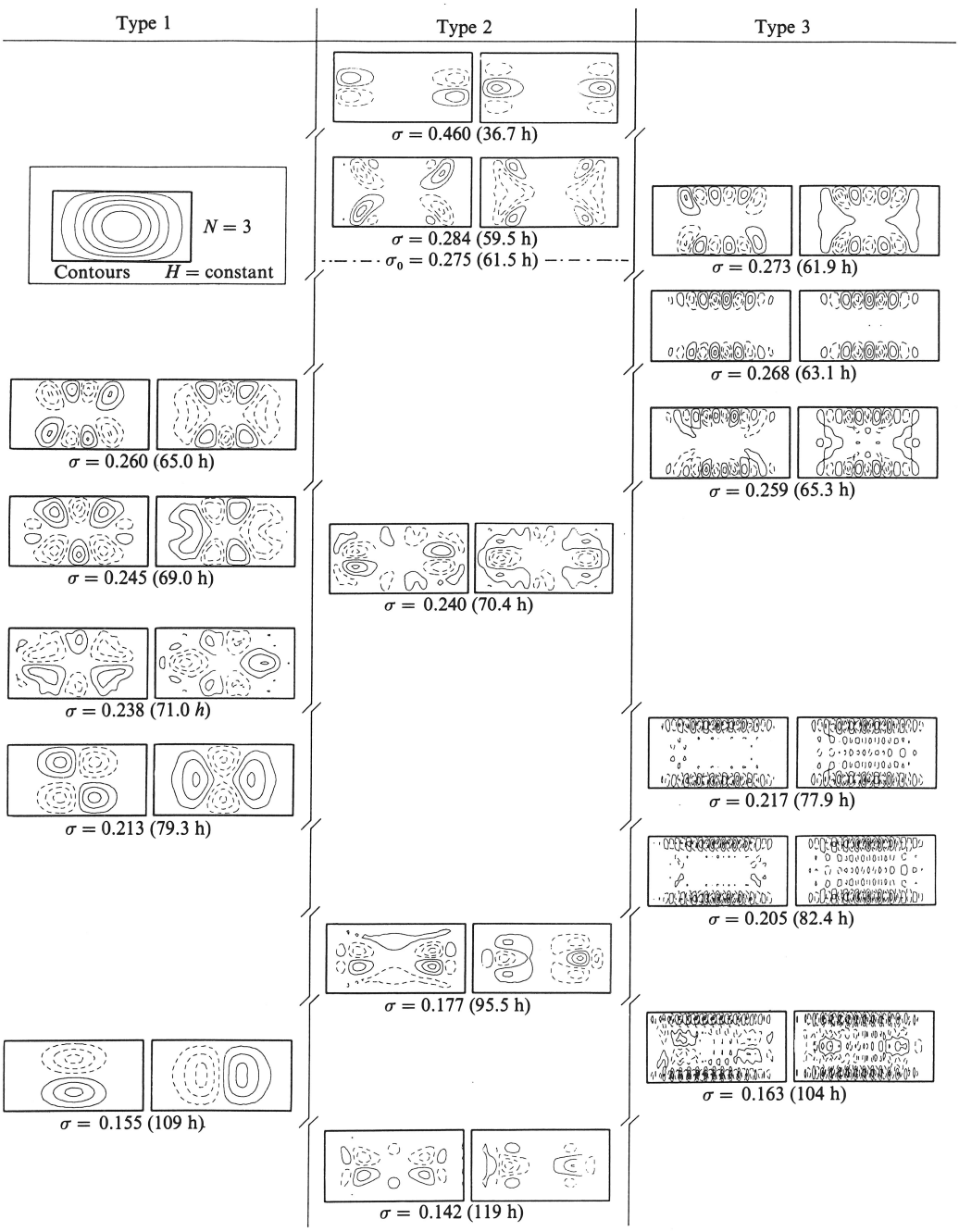

FIGURE 3. Same as figure 2 for a third-order model $N = 3$.

Ball mode occur in the spectrum, and additional eigenmodes are identified as type 1. All exact models existing so far, have shown qualitatively similar solutions. Generally, Ball modes consist of a few largescale vortices moving counterclockwise (on the northern hemisphere) around the basin and the water in the whole basin underlies this wave motion.

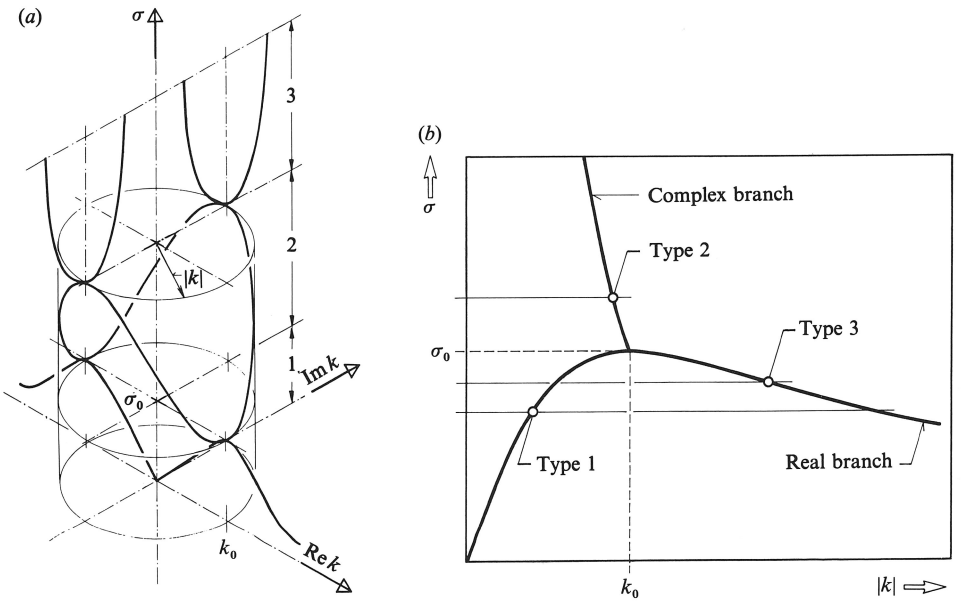

FIGURE 4. (*a*) Schematic plot of one mode unit of the dispersion relation of topographic waves in an infinite channel. An Nth-order model consists of N mode units, each of which exhibits three regimes where the wavenumbers are real, complex and imaginary, respectively. (*b*) An enlarged portion of (*a*). Type 2 modes occur above the cutoff frequency σ_0.

Type 2, with only a few candidates in this frequency interval, can be called *bay-type*. Wave motion is mostly trapped at the long ends of the lake; very weak activity is experienced in the lake centre and along its long sides. The pattern shows one or more midscale gyres which do not propagate along the entire isobaths (lines of constant f/H) but are rather trapped in the bays. This type arises above the cutoff frequency σ_0 for topographic waves in an infinite channel (see below) and thus embraces contributions with non-real wavenumbers. This is a new result, and these modes were neither detected by the analytic models nor by the crude lake model (channel with vertical endwalls) proposed by Stocker & Hutter (1986).

Type 3, eventually, appears most frequently in the spectrum. Along the long boundaries of the basin a large number of small-scale vortices is observed. The pattern is very similar to that found in straight infinite channels and in elongated lakes, see Johnson (1987*b*); type 3 is thus named *channel-type*.

The modal structure and related properties of the different types can easily be explained with the help of the Rossby dispersion relation. Figure 4(*a*) displays one mode unit of the dispersion relation of topographic wave propagation in an infinite channel. Summarizing the results of Stocker & Hutter (1986) we mention that each wave mode is associated with a mode unit consisting of three subsequent regimes: for $\sigma < \sigma_0$ the wavenumbers are real and $\sigma(k)$ takes the familiar form with a critical point (σ_0, k_0) where the group velocity is zero; for $\sigma > \sigma_0$ the wavenumbers take complex values accounting for an exponential decay or growth of the stream function in space; in the third regime k is purely imaginary. Regime 1 and partly regime 2 are enlarged in figure 4(*b*). As is obvious from figures 2 and 3, type 1 enjoys the property that increasing σ brings about more spatial structure. It follows that this type consists primarily of modes with wavenumbers $k < k_0$. For $k < k_0$, $\partial\sigma/\partial k > 0$ and so

the wavelengths of the contributing modes decrease with growing σ. Type 3, on the other hand, reveals the opposite property: the scale of the wave pattern gradually decreases with decreasing frequency. These solutions are mostly made up of modes with $k > k_0$. In this range, $\partial\sigma/\partial k < 0$ and consequently the wavelengths decrease with decreasing σ.

The findings of Johnson (1987*b*) substantiate the above statements. His approximate model of an elongated basin allows calculation of eigensolutions which simply evolve from a quantization of the wavenumber k of the dispersion relation $\sigma(k)$ of the infinite channel. Modes termed here as Ball-types are characterized there similarly by $0 < k < k_0$, whereas channel-types have $k > k_0$. Mathematically, a distinction of these two types, therefore, is not compelling.

The existence of eigenmodes above the cutoff frequency σ_0 is a new result. Modes in this regime have complex wavenumbers and this explains why bay-type waves show the conspicuous structure. Wave activity is close to the lake ends, and away from it is exponentially evanescent. It remains an open question whether there exist super-inertial eigenmodes with $\sigma > 1$ or $\omega > f$. These modes could interfere with gravity waves and the low-frequency approximation (which led to (2.1)) is not appropriate any longer. A test has shown that a model with $N = 2$ and the parameters given in figure 2 has no eigenfrequencies in the interval $0.5 < \sigma < 4$.

The physical consequences of these bay-types are further discussed in 3.3. The occurrence of bay-trapped modes casts light on recent finite element results (Trösch 1984) of topographic waves in the northern part of the Lake of Lugano. These seemed to contradict entirely the applicability of analytic models to real basins because fundamental modes (Ball modes) were not found in the 65 h–120 h period interval. They showed rather small-scale eigenmodes (akin to type 3) and, more interesting, modes (akin to type 2) which were clearly trapped to the three Bays of Melide, Lugano and Porlezza, respectively. Figure 5 shows three of these bay-type solutions in the period domain of interest. Each mode is trapped in one of the bays not influencing the rest of the basin and the few vortices exhibit roughly the scale of the bay. The rectangular basin, a much simpler configuration than the Lake of Lugano, reveals equally bay-type modes together with the known Ball-type solutions which in the interested period range were not found by Trösch (1984). This model, therefore, links these two different approaches, and demonstrates that the propagation of topographic waves in enclosed basins cannot be described merely by the exact models which exist so far. The rectangular basin incorporates two features which seem to be crucial for the analysis of topographic waves. As with all exact models, it has continuous depth contours which are vital for the existence of the Ball-type modes. Moreover, the exact models all have boundary lines which are similar to the depth contours. The boundary of the finite-element model of the Lake of Lugano, however, incorporates bays and global curvature, which destroy similarity and smoothness; the rectangular basin lacks similarity of the shore line and isobaths as well. This is likely to make the existence of the bay-type possible.

3.2. *Convergence and parameter dependence*

This model is merely an approximation because of the truncation of the series expansion at some finite N. Its quality strongly depends on the type of wave considered. It is only the transverse variability which is limited for a given order N, whereas the solution is well represented along the lake axis by virtue of the Runge–Kutta scheme. Ball-type modes have large-scale vortices, and a good

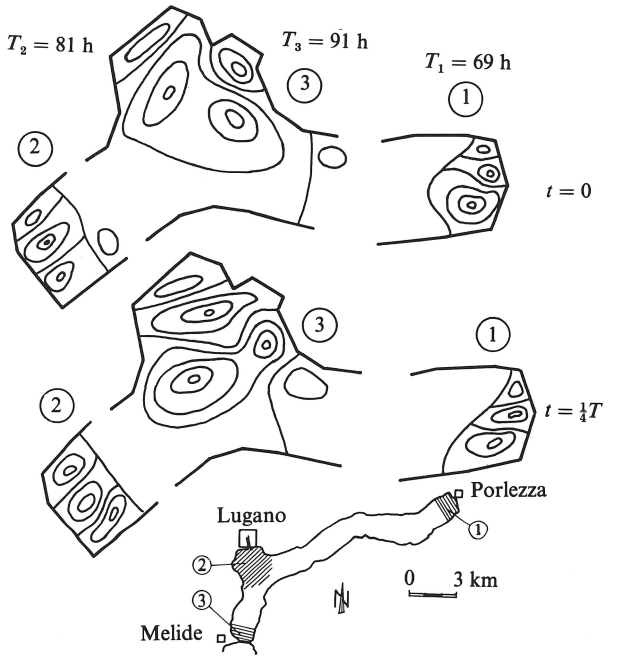

FIGURE 5. Three modes of topographic waves in the northern part of the Lake of Lugano from finite element calculations by Trösch (1984). The wave motion is trapped in the three bays shaded in the inset.

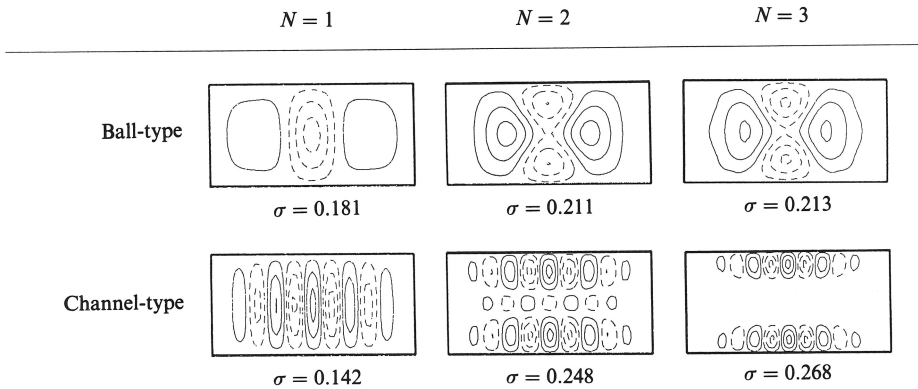

FIGURE 6. Convergence of both, eigenfrequency and stream function of the quadratic Ball mode and a channel mode. The parameters are as in figure 2.

representation of these modes with comparatively few basis functions is expected. High orders of expansions are therefore not needed; fast convergence is observed. By contrast channel-type solutions consist of small-scale modes with large wavenumbers. As was shown in Stocker & Hutter (1986) convergence is slower for large wavenumbers and this must equally be expected for type 3 modes.

Figure 6 demonstrates convergence of both eigenfrequency and stream function for the quadratic Ball mode and one-channel mode. Qualitative changes when increasing $N = 1$ to $N = 2$ regarding the stream function are observed. Whereas the lowest-order model predicts a coherent central gyre for the Ball-type, it splits into

	$N = 1$	$N = 2$	$N = 3$
Ball-type	0.143	0.153*	0.155*
	0.181	0.211*	0.213*
	0.195	0.255*	0.260*
Channel-type	0.151	0.254*	0.273*
	0.142	0.248*	0.268*
	0.111	0.215*	0.253

TABLE 1. Convergence of three selected eigenfrequencies in a basin with $q = 2.0$, $\epsilon = 0.05$, $\eta = 0.01$ for the Ball- and channel-type. Asterisks indicate plotted modes in figures 2 and 3.

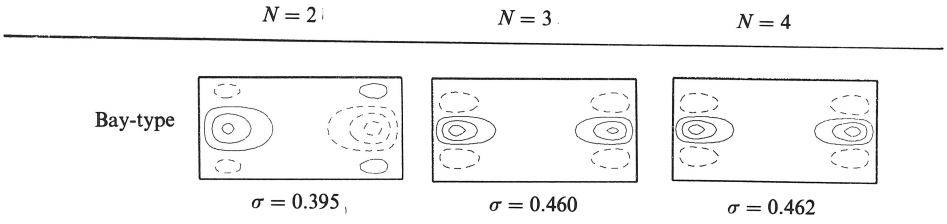

FIGURE 7. Converging eigenfrequency and stream function of a bay mode. The parameters are as in figure 2.

	$N = 2$	$n = 3$	$N = 4$
Bay-type	0.395	0.460	0.462
	0.297	0.314	0.318
	0.263	0.284	0.293
	0.115	0.240	0.251

TABLE 2. Convergence of the eigenfrequencies of four selected bay modes. The parameters are as in table 1.

two vortices for higher orders. Equally, the first-order model yields mass transport across the lake basin and thus a strong interaction of the two lateral beat patterns of the channel-type. This is lifted as N increases, and $N = 2$ already shows two nearly independent structures. Table 1 gives the eigenfrequency for some more modes of the Ball- and channel-type. It is consistent with the properties of the dispersion relation that convergence is slower as σ decreases.

It is of particular importance to test convergence for the new bay mode. This is shown in figure 7 and table 2. Bay modes for $N = 1$ were not found and convergence is studied for models up to $N = 4$. For $N = 3$ good estimates have been achieved for both the eigenfrequency and the stream function. It is characteristic of the bay mode that it has very small values of ψ in the central area of the basin. Comparing it for $N = 2$ and $N = 3$ we observe that the solutions exhibit a different parity with respect to the lake centre. Moreover, for higher orders the pattern was only obtained by a forward and backward integration from $s = 0$ and $s = L$, respectively. The stream function of the bay mode is strongly attenuated in the centre and hence the basic problem is to bring numerical information through the 'dead' zone towards the opposite end of the lake. Perhaps the use of a multi-step integration scheme would bring some improvement.

Ball quadratic	$r = 0.5$	$r = 0.4$	$r = 0.3$
$q = 1.0$	0.267	0.250	0.219
$q = 2.0$	0.211	0.195	0.170
$q = 5.0$	0.140	0.123	?

TABLE 3. Topography q and aspect ratio r influencing the eigenfrequency of the quadratic Ball mode. The parameters are $N = 2$, $\epsilon = 0.05$, $\eta = 0.01$.

$r = 0.5$	Ball-type	Bay-type	Channel-type
$q = 1.0$	0.200	0.299	0.250
$q = 2.0$	0.153	0.395	0.232
$q = 5.0$	0.097	0.415	0.153

TABLE 4. Topography effect on the frequency of the three wave types. The parameters are as in table 3.

$q = 2.0$	Ball-type	Bay-type	Channel-type
$r = 0.5$	0.153	0.263	0.232
$r = 0.4$	0.139	0.267	0.251
$r = 0.3$	0.118	0.269	0.258

TABLE 5. Aspect ratio effect on the frequencies of the three types. The parameters are as in table 3 and the case $r = 0.5$ matches table 4 with $q = 2.0$.

We next study the influence of the topography parameters q and the aspect ratio r on the eigenfrequencies of the different modal types. Table 3 collects the results for the solutions that correspond to Ball's quadratic mode. As expected from the behaviour of the dispersion relation in a straight infinite channel the shape of the transverse topography has a dominant influence on the values of the eigenfrequency. Steeper profiles ($q = 5.0$) lower the eigenfrequencies as q governs the value of σ_0. An equal but weaker effect on Ball-type modes is experienced when the aspect ratio is decreasing. Table 3 demonstrates that these modes are much more governed by the transverse depth profile than by the aspect ratio.

Tables 4 and 5 investigate the influence of the two bathymetric parameters q and r on the three wave types. Again the topography effect (table 4) is seen to be more influential. By going from a triangular depth profile ($q = 1.0$) k to a very steep U-shaped profile ($q = 5.0$) the eigenfrequencies diminish by up to a factor of 2. As far as the topography effect is concerned, the Ball and channel types react the same way, whereas the eigenfrequencies of the bay-type modes increase weakly with q.

Table 5 shows that basins with a smaller aspect ratio sustain Ball-type waves with decreased eigenfrequencies. This decrease is over-proportional as it is enhanced for smaller aspect ratios. By contrast, bay- and channel-type solutions exhibit the opposite behaviour. Decreasing the aspect ratio increases the eigenfrequency; this time the response is under proportional and for bay-type solutions the dependence of σ on r is very small.

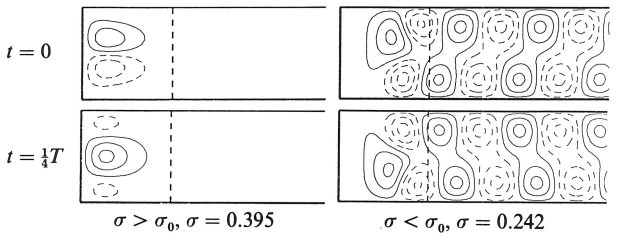

FIGURE 8. Reflection patterns for $\sigma > \sigma_0$ and $\sigma < \sigma_0$ in a semi-infinite channel with the depth profile (3.1) and $s = s_0$ is indicated by the dashed vertical line. For $\sigma > \sigma_0$ the solutions are bay-trapped and spatially evanescent. Frequency and wave pattern coincide with the mode on the top of figure 2. The parameters are as in figure 2.

3.3. *The bay-type, further remarks*

The occurrence of bay-trapped modes in enclosed basins was unexpected and raises further questions concerning the properties of solutions of the eigenvalue problem (2.1).

When the aspect ratio of the basin is decreased the bay vortices of these modes lie farther and farther apart and we wonder whether these isolated gyres become uncoupled. There are two points to be remarked upon. First, basins with no symmetry seem to sustain decoupled bay-modes as in figure 5; finite element calculations point in this direction. Secondly, with our procedure it is very difficult to determine the parity of these solutions with respect to the long axis of the basin. In this direction very fine resolution is needed to obtain reliable solutions. This problem was addressed above and the results suggest considering again semi-infinite channels as was done in earlier work (Stocker & Hutter 1986). It is now proposed to model the bay-section of the semi-infinite channel by a $\sin^2$–thalweg profile; lines of f/H = constant are continuous and differentiable. Results are presented in Stocker & Hutter (1987) and Stocker (1987) we only anticipate those relevant in this context. Applying the same shooting method to the composed channel-axis depth profile

$$h(s) = \begin{cases} \eta + \sin^2\left(\dfrac{\pi s}{2s_0}\right) & (0 < s < s_0), \\ \eta + 1 & (s \geqslant s_0), \end{cases} \tag{3.1}$$

solves the problem of topographic wave reflection in a semi-infinite channel. Recall, that for $\sigma > \sigma_0$, freely propagating waves are not allowed in the domain $s \geqslant s_0$ of the infinite channel. It therefore came as a surprise to find non-trivial solutions above the cutoff frequency. This is shown in figure 8; contour lines of two solutions are plotted for $t = 0$ (above) and $t = \frac{1}{4}T$ (below) belonging to the regimes $\sigma > \sigma_0$ (left) and $\sigma < \sigma_0$ (right), respectively. The latter agree with the solutions of Johnson (1987*b*). The typical bay-trapped structure is visible and due to contributions of modes with only complex wavenumbers in $s > s_0$, i.e. the stream function is exponentially evanescent there. Calculations have demonstrated that such solutions only exist for particular frequencies. For $\sigma < \sigma_0$, however, every frequency sustains a free wave with real wavenumbers forming true reflection pattern. At $\sigma = 0.115$, a frequency below σ_0 exceeding, however, the cutoff of the second mode unit, a further bay-mode

appears (not shown in figure 8). Weak wave activity in the region of uniform depth $s > s_0$ gives rise to strong wave motion in the shore-zone $s < s_0$. This mode corresponds to the bay-mode at the same frequency in figure 2. The spectrum of the semi-infinite channel thus embraces both a discrete and continuous part. It turns out that the discrete spectrum is identical to the spectrum of the bay-type modes with $\sigma > \sigma_0$ of the rectangular basin, see figure 2.

Physically, these modes have the character of resonances of the system, and a bay-type mode in the rectangular basin can then be interpreted as the superposition of two resonances at either lake end. The longer a basin is, the weaker will be the interaction of the individual bays, which confirms the above conjecture. Eventually, a bay in an elongated lake can sustain its individual and isolated bay-mode. This agrees with the results in figure 5 and settles the former controversy. It also explains the very weak dependence of the bay mode on the aspect ratio which is a global measure of the lake basin. Bay modes will rather depend on the local geometry of the sustaining bay. This is a result which can already be inferred from figure 5.

4. Conclusions

The channel models, derived using the Method of Weighted Residuals and being an effective tool in solving the problem of topographic wave motion in straight infinite channels, were applied to rectangular basins with continuous depth lines. The partial differential equation in two spatial dimensions was transformed into a system of ordinary differential equations with non-constant coefficients, the size of which depended on the order of the transverse functional expansion. This system was solved by applying a Runge–Kutta scheme and the eigenfrequencies and associate stream functions were found by satisfying a no-flux condition at the far end of the basin.

Three qualitatively different types of solutions were discovered: Ball-, bay- and channel-type. The occurrence of modes with a few large-scale vortices is well known and was expected from results of earlier analytic models such as Ball (1965), Johnson (1987*b*) (small wavenumbers) and others. In addition, channel-type solutions consisting of many small-scale vortices were found. These are akin to those emerging in the model of Johnson (1987*b*) (large wavenumbers). The spectrum, however, incorporates yet another type of solution. Wave activity can be trapped in the bays of the lake in the form of a few midscale gyres. This bay type arises at frequencies above the cutoff of the individual mode units and a qualitative agreement with finite element solutions is found.

The investigation of bay modes in semi-infinite channels with smooth depth-lines has brought more understanding of the trapping mechanism. A bay mode is then interpreted as being a resonance of the sustaining system. This makes it clear why all previous analytical models have not given an indication of the existence of bay modes. Since in these, shorelines and isobaths are similar, there is no distinct and localized region within the basin which could act as a resonator. Therefore, resonances and with it bay modes are unlikely to occur. These basins were, however, very special configurations scarcely found in nature. In a real lake with curvature and bays it has to be reckoned that each bay can sustain its own mode.

From an experimental point of view this finding is equally important. The three types can have similar frequencies which are difficult to discern. In spite of their spectral proximity they exhibit distinctly different transport patterns and particle

paths. It follows that a very accurate knowledge of the time evolution of the velocity vector is required in order to distinguish clearly the individual types.

Further properties of the bay mode and a unified classification of the three types in terms of topographic wave reflection are the topic of current research.

We thank I. Wiederkehr and C. Bucher for preparing the drawings.

REFERENCES

BALL, F. K. 1965 Second class motions of a shallow liquid. *J. Fluid. Mech.* **23**, 545–561.

BÄUERLE, E. 1986 Eine Untersuchung über topographische Wellen in einem Kanalmodell. *Mitteilungen der Versuchsanstalt für Wasserbau, Hydrologie und Glaziologie. ETH Zürich*, No. 83.

FINLAYSON, B. A. 1972 *The Method of Weighted Residuals and Variational Principles.* Academic.

HUTTER, K., SALVADÈ, G. & SCHWAB, D. J. 1983 On internal wave dynamics in the northern basin of the Lake of Lugano. *Geophys. Astrophys. Fluid Dyn.* **27**, 299–336.

HUTTER, K. & VISCHER, D. 1986 Lake Hydraulics. In *Developments in Hydraulic Engineering* (ed. P. Novak), vol. 4. Elsevier.

JOHNSON, E. R. 1987*a* Topographic waves in elliptical basins. *Geophys. Astrophys. Fluid Dyn.* **37**, 279–295.

JOHNSON, E. R. 1987*b* A conformal mapping technique for topographic-wave problems: semi-infinite channels and elongated basins. *J. Fluid Mech.* **177**, 395–405.

LAMB, H. 1932 *Hydrodynamics*, 6th edn. Cambridge University Press.

MYSAK, L. A. 1985 Elliptical topographic waves. *Geophys. Astrophys. Fluid Dyn.* **31**, 93–135.

MYSAK, L. A., SALVADÈ, G., HUTTER, K. & SCHEIWILLER, T. 1985 Topographic waves in an elliptical basin, with application to the Lake of Lugano. *Phil. Trans. R. Soc.* A **316**, 1–55.

SAYLOR, J. H., HUANG, J. S. K. & REID, R. O. 1980 Vortex modes in southern Lake Michigan. *J. Phys. Oceanogr.* **10**, 1814–1823.

STOCKER, T. 1987 A theoretical study of topographic wave reflection in estuaries. *J. Phys. Oceanography* (submitted).

STOCKER, T. & HUTTER, K. 1986 One-dimensional models for topographic Rossby waves in elongated basins on the *f*-plane. *J. Fluid Mech.* **170**, 435–459.

STOCKER, T. & HUTTER, K. 1987 *Topographic waves in channels and lakes on the f-plane.* Lecture Notes on Coastal and Estuarine Studies, vol. 21. Springer.

TRÖSCH, J. 1984 Finite element calculation of topographic waves in lakes. *Proc. 4th Intl Conf. on Applied Numerical Modeling, Tainan, Taiwan.*